POLITECNICO MILANO 1863

SCUOLA DI INGEGNERIA INDUSTRIALE E DELL'INFORMAZIONE

Executive Summary of the Thesis

Techno-Economic Assessment and Optimal Sizing of a High-Temperature Heat Pump Configuration for Geothermal District Heating Applications

Laurea Magistrale in Energy Engineering - Ingegneria Energetica

Author: Alice Rossi

Advisor: Prof. Dario Alfani

Co-advisors: Prof. Christopher Schifflechner, Arianna Passamonti

Academic year: 2025-2026

1. Introduction

The decarbonisation of the heating sector is one of the central challenges of the energy transition, as a large share of the thermal demand is still met by fossil fuels. In Germany, the heating and cooling sector accounts for roughly 26% of final energy consumption, and in 2023 about 70% of the national thermal demand was still supplied by fossil sources [1]. In this context, high-temperature heat pumps (HTHPs), able to deliver supply temperatures up to 100 °C, coupled to renewable energy-supplied district heating networks (DHNs), represent a promising route to greenhouse-gas abatement, particularly when a geothermal source is available as the low-temperature heat input.

Although the integration of heat pumps into geothermal DHNs has been studied extensively, most of the literature addresses a single cycle topology, a restricted set of working fluids, or design-point calculations rather than full annual simulations. A systematic comparison of several cycle architectures under identical boundary conditions, with simultaneous low-GWP refrigerant screening and compressor sizing, is still lacking.

This work addresses this gap through a techno-economic assessment of a large-scale HTHP integrated into the geothermal DHN of the Isar Valley (Molasse Basin, Germany). Three cycle architectures, shown in Figure 1, are compared on the same real application:

- a single-stage cycle (SS);
- a single-stage cycle with internal heat exchanger (SS+IHX), i.e. with a recuperator;
- a two-stage cascade cycle.

For each configuration a screening of several low-GWP working fluids is performed, the minimum compressor size covering the peak thermal demand is determined, and the annual performance is evaluated through a 8760-hour thermodynamic simulation. A scalability analysis is then carried out progressively reducing the installed heat pump power, and assigning the residual load to an auxiliary natural gas boiler, in order to identify the optimal system sizing. The configurations are compared through the coefficient of performance (COP), the annual electricity consumption, the equivalent full-load operating hours, and the levelised cost of heat (LCOH).

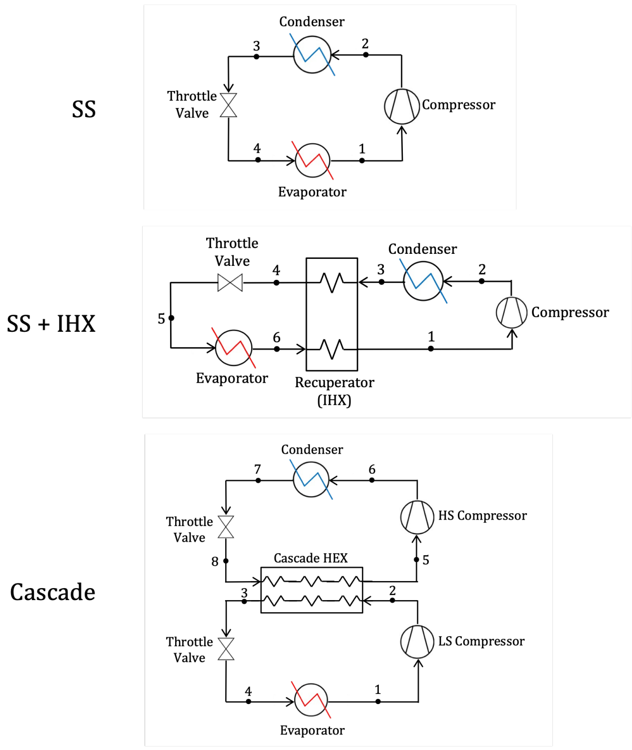

Figure 1: Schematic representations of the three HTHP cycle configurations: SS, SS+IHX, cascade.

2. Reference system and methodology

2.1. Reference system

The heat source is the geothermal brine extracted from the Molasse Basin at an average depth of 4000 m, reaching the surface at 90 °C to 110 °C with a total mass flow rate of 81.5 kg/s. After the primary heat exchanger, the brine enters the heat pump cycle at 61.5 °C in the maximum load condition, and its return temperature is kept above 30 °C to prevent thermal depletion of the reservoir. The heat pump condenser delivers a nominal thermal output of 7.13 MW to the DHN, which operates with a supply temperature between 56.5 °C and 93.6 °C. The annual load profile is derived from the measured demand of an existing plant in the same area combined with hourly ambient temperature data for Munich (April 2022 – March 2023). It should be noted that the geothermal production system, the primary heat exchanger, the district heating network, and the auxiliary natural gas boiler are regarded as predefined system components and are therefore not subject to redesign within the scope of this work. The objective of the present study is exclusively the thermo-economic sizing and assessment of the high-temperature heat pump to be integrated into this existing infrastructure.

2.2. Refrigerant selection

Candidate fluids must combine a high critical temperature, a critical pressure below 30 bar, an evaporation pressure above 1 bar, low GWP and zero ODP, and acceptable safety and cost [3]. Guided by the literature and based on these criteria, six low-GWP refrigerants were retained, spanning hydrofluoroolefins (HFOs), a hydrochlorofluoroolefin (HCFO) and hydrocarbons (HCs), as summarised in Table 1.

Table 1: Selected working fluids and thermophysical properties.

Type	Refrigerant	T_c [°C]	p_c [bar]	MM [g/mol]	Price [€/kg]
HFO	R1234yf	94.7	33.8	114.0	20
HC	Propane	96.7	42.5	44.1	2
HC	Isobutane	134.7	36.3	58.1	2
HFO	R1234ze(Z)	150.1	35.3	114.0	20
HC	Butane	152.0	38.0	58.1	2
HCFO	R1233zd(E)	166.5	36.2	130.5	35

2.3. Modelling assumptions

The steady-state cycle model, based on the framework of Kaufmann et al. [5], defines the source and load boundary conditions for each hourly operating point and retrieves thermophysical properties from REFPROP [6]. For every operating condition the problem is formulated with two decision variables, the working fluid mass flow rate $\dot{m}_{HP}$ and the evaporation pressure p_{evap}, chosen to minimise the compressor mechanical power while exactly meeting the DHN thermal load, subject to a minimum 5 K pinch point on all heat exchangers and a compressor speed within 500 rpm to 4500 rpm.

The twin-screw compressor is described with the generalised low-order approach of Kaufmann et al. [4], which returns the isentropic and volumetric efficiencies as functions of the normalised suction flow rate and pressure ratio, thereby enabling realistic part-load modelling. The heat exchangers are modelled with a finite-volume energy-balance approach.

In the SS+IHX configuration the recuperator is not imposed through a fixed subcooling, but through a specified pinch-point temperature difference ΔT_{rec} linking the compressor inlet (state 1) to the hot-side outlet (state 3):

$$T_1 = T_3 - \Delta T_{rec}, \tag{1}$$

with the resulting superheating obtained from the recuperator energy balance rather than assigned. In the cascade cycle the intermediate temperature level is set through a weighting factor $w_{LS} \in [0, 1]$ that redistributes the total lift between the two stages:

$$T_{switch} = (1 - w_{LS})\, T_{evap,LS} + w_{LS}\, T_{cond,HS}, \tag{2}$$

and it is optimised to minimise the total annuities.

2.4. Economic model

Component CAPEX is estimated with exponential scaling correlations, and annual costs are computed with the annuity method following VDI 2067 [2], distinguishing a capital-bound annuity AN_K, a demand-bound annuity AN_V (electricity for the heat pump, natural gas for the boiler) and an operation-bound annuity AN_B (maintenance, 2.5 % of CAPEX/y). The system levelised cost of heat combines the heat pump and boiler annuities over the total useful heat delivered:

$$\mathrm{LCOH}_{sys} = \frac{AN_{HP} + AN_{Boiler}}{Q_{HP} + Q_{Boiler}}. \tag{3}$$

The economic boundary is limited to the heat pump and the operating cost of the auxiliary boiler. A baseline scenario (mean gas price 47.3 €/MWh, no CO_2 cost, mean electricity price 133.6 €/MWh) is complemented by a sensitivity analysis over representative gas, electricity and carbon-price scenarios. The discounted payback time (PBT) is adopted as a complementary economic indicator: it measures the number of years after which the cumulative discounted savings, evaluated as the difference in operating cost between the all-boiler reference case and the integrated heat-pump-plus-boiler system, offset the additional heat pump investment.

3. Results

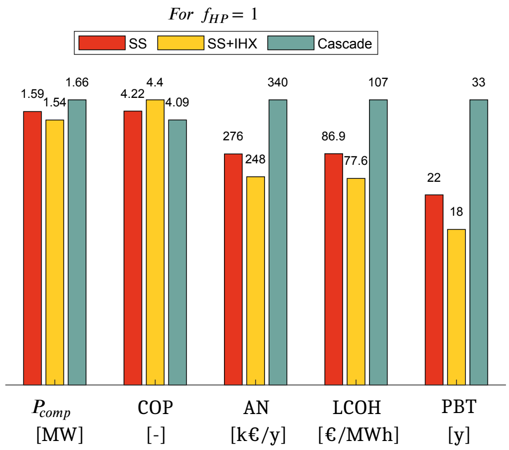

Figure 2: Comparison of the three cycle configurations across the main thermodynamic and economic indicators at the design point

3.1. Comparison of the configurations

The three architectures deliver comparable thermodynamic performance at the design point but differ markedly on the economic side. The introduction of the recuperator improves the COP of every refrigerant with respect to the SS cycle, while adding only a limited investment: the IHX accounts for less than 7 % of the heat pump capital cost across the whole sizing range. The two-stage cascade, by contrast, is not competitive for this application: at the moderate temperature lift of this geothermal source, the thermodynamic benefit of two-stage compression, which becomes significant only for large lifts, does not offset the cost of the second compressor and the cascade heat exchanger. This is summarised in Figure 2, which compares the three architectures across the main indicators: the SS+IHX cycle attains the lowest total annuity and, consequently, the lowest LCOH (77.6 €/MWh, against 86.9 €/MWh for the SS cycle and 107 €/MWh for the cascade). In addition, the SS+IHX cycle amortises the heat pump investment in approximately 18 years under baseline prices, the shortest of the three configurations.

Across all configurations, hydrocarbons consistently provide the best economic performance, combining a competitive COP with a low capital cost. In the SS+IHX cycle isobutane (R600a) achieves the lowest LCOH, closely followed by butane (R600); the two fluids differ by less than 2 % and thus they can be regarded as essen-

tially equivalent from an economic perspective. Table 2 reports the design-point results for the SS+IHX configuration.
For isobutane, the recuperator pinch point was optimised as a trade-off between annual efficiency and cost: high ΔT_{rec} penalises both the design-point and the demand-weighted annual COP, whereas the annuity and LCOH follow a minimum-seeking trend. The value $\Delta T_{rec} =$ 11 K minimises the LCOH (with the lowest annuity, ≈ 248 k€/y) and is therefore adopted. On the basis of this comparison, the SS+IHX cycle with isobutane is selected as the reference scenario for the sizing study.

3.2. Optimal heat pump sizing

The installed heat pump power is then progressively reduced through a sizing factor f_{HP}, with the residual load met by the boiler. Because the annual heat delivered to the network is essentially independent of f_{HP}, the system LCOH mirrors the non-monotonic behaviour of the total annuity: it first decreases, as cheap heat-pump electricity displaces expensive boiler gas, and then rises again as the growing CAPEX and electricity consumption outweigh the marginal gas savings. Under the baseline scenario the LCOH reaches its minimum of about 72.0 €/MWh at $f_{HP} \approx 0.4$ (Figure 3).

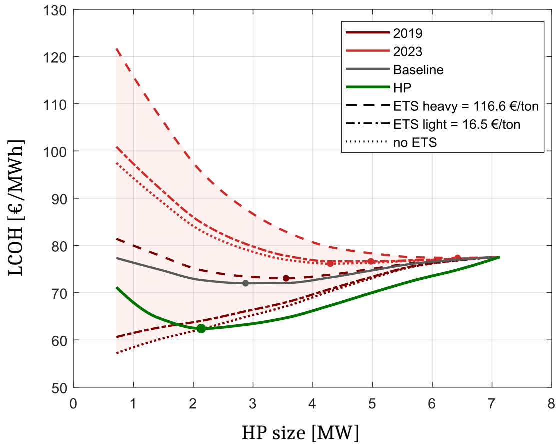

Figure 3: System LCOH as a function of the heat pump size for different natural gas price and CO_2 emission cost scenarios; the green curve reports the levelised cost of the heat pump alone.

However, the purely economic optimum yields a modest renewable coverage (about 73 % of the annual demand) as shown in Figure 4. Owing to the flat-bottomed shape of the LCOH curve, increasing the sizing factor to $f_{HP} \approx 0.6$ raises the LCOH by less than 2 % (to 73.2 €/MWh) while increasing renewable coverage from 73 % to 89 % (Figure 4) and almost eliminating the direct CO_2 emissions of the boiler (from 540 ton/y at $f_{HP} = 0.1$ to 79 ton/y). Beyond this size, further increments displace only a marginal residual boiler contribution at the expense of a disproportionate rise in the HP investment cost. A sizing factor of approximately 0.6 is therefore identified as the most advantageous compromise between economic competitiveness, high renewable coverage, and adequate heat pump utilisation.

Table 2: Comparison of refrigerants in SS + IHX at nominal point

Refrigerant	$\dot{m}_{HP}$ [kg/s]	p_{evap} [bar]	V_s [m^3]	ΔT_{rec}^{opt} [K]	P_{compr} [MW]	$\dot{Q}_{evap}$ [MW]	COP [-]	CAPEX [k€/y]	AN [k€/y]	LCOH [€/MWh]
R1234ze(Z)	34.2	2.9	0.041	9	1.5	5.63	4.5	70	284	88.3
R1233zd (E)	37.6	2.14	0.0595	13	1.48	5.64	4.55	93	345	103.5
R600	20.13	3.7	0.0382	13	1.5	5.6	4.53	58	256	79.1
R600a	21.9	5.3	0.028	11	1.52	5.61	4.45	54	248	77.5
R290	24.3	14	0.0164	7	1.84	5.3	3.67	39	258	79.6

R1234yf results are not available because of the low critical temperature.

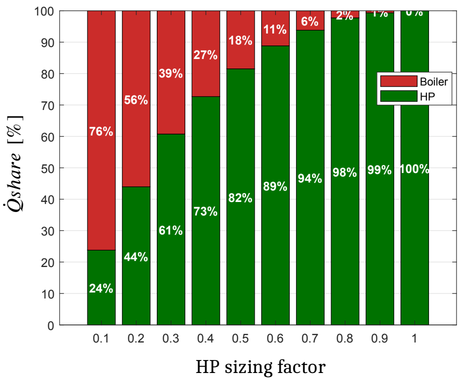

Figure 4: Distribution of the annual heat production between the heat pump and the auxiliary boiler for different sizing factors.

3.3. Sensitivity analysis

A sensitivity analysis was then carried out by varying both the natural gas price and the electricity price across representative scenarios; the results are reported in Figure 5, organised into three panels, each corresponding to a different electricity price scenario (left: 2019; centre: 2022; right: mean). The electricity price scenario affects not only the absolute level of the system LCOH, lower electricity prices yield proportionally lower curves,but also the location of the economic optimum.

The optimal heat pump size is governed not by either energy price in isolation, but by their ratio. Consequently, the optimal size increases monotonically with this ratio:

- within a fixed gas scenario, lowering the electricity price raises the ratio and shifts the optimum towards larger sizes;
- within a fixed electricity scenario, lowering the gas price reduces the ratio and shifts the optimum towards smaller sizes;
- matching-tier scenarios (gas and electricity both at their 2019, mean, or high levels) leave the ratio approximately unchanged and share a common optimum near 2.9 MW, whereas a one-tier mismatch in favour of gas shifts it to approximately 4.3 MW;
- when gas is cheap and electricity expensive, the unconstrained optimum falls below the smallest simulated size, so that several price pairs collapse onto the lower bound of approximately 0.7 MW.

The heat-pump-only curve, by contrast, retains its minimum at approximately 2.1 MW regardless of scenario, since by excluding the boiler gas expenditure it is insensitive to the price ratio. Although the absolute levelised cost and the precise location of the optimum depend appreciably on the energy-price scenario, the flat-bottomed shape of the LCOH curves implies that a sizing factor of approximately 0.6 entails only a marginal economic penalty across the full range of plausible market conditions, while securing a substantially higher renewable coverage. The selected sizing factor is thus retained as a robust compromise—not because the economic optimum is stationary, but because the cost surface is shallow around it.

4. Conclusions

This work presented a techno-economic assessment and optimal sizing study of a large-scale high-temperature heat pump integrated into the geothermal district heating system of the Isar Valley. Three cycle architectures: single-stage, single-stage with internal heat exchanger, and two-stage cascade, were compared under identical boundary conditions, each coupled with a low-GWP refrigerant screening, an annual 8760-hour simulation, and a unified LCOH-based economic evaluation including an auxiliary natural gas boiler. The main findings are:

- The **SS+IHX cycle** emerges as the most favourable compromise between cycle efficiency and capital expenditure. The recuperator improves the COP of every fluid while adding less than 7 % to the heat pump CAPEX, whereas the cascade cycle is penalised by its higher component count at the moderate lift of this application. The discounted payback time confirms the selection of the SS+IHX configuration, amortising the investment in about 18 years under baseline prices and dropping to roughly 5 years once CO_2 pricing is accounted for, well within the plant lifetime.
- **Hydrocarbons** give the best economics. Isobutane (R600a) yields the lowest preliminary LCOH (77.5 €/MWh), with a design-point COP of 4.45 and an optimal recuperator pinch point of 11 K; butane is essentially equivalent.
- A **sizing factor** ≈ 0.6 is the most advantageous compromise: it raises the LCOH

by less than 2 % above its minimum while lifting renewable coverage from 73 % to 89 % and nearly eliminating boiler emissions. This choice is robust to energy-price assumptions owing to the flat-bottomed LCOH curves, even though the absolute optimum shifts with the gas-to-electricity price ratio.

The analysis is subject to some limitations that also indicate directions for further work. The economic boundary excludes the boiler CAPEX, well drilling, the brine pump and the primary heat exchanger; so this simulation framework is not adapt to assess completely new installations. Furthermore, the model is steady-state and typeday-based, so transient and part-load control effects are not captured; and the refrigerant and cascade-pairing screening could be extended. The integration of thermal energy storage, a reversible operating mode, and future energy- and carbon-price scenarios represent promising extensions that could further improve the decarbonisation potential of the integrated system.

5. Acknowledgements

The author wishes to thank the advisor Prof. Dario Alfani and the co-advisors Prof. Christopher Schifflechner and Arianna Passamonti from Technical University of Munich for their guidance and support throughout this work.

References

[1] Energy Statistics Data Browser – Data Tools - IEA.

[2] VDI - The Association of German Engineers. Economic efficiency of building installations - Fundamentals and economic calculation. (VDI 2067 Blatt 1). DIN Media GmbH; 2012.

[3] Cordin Arpagaus, Frédéric Bless, Michael Uhlmann, Jürg Schiffmann, and Stefan S. Bertsch. High temperature heat pumps: Market overview, state of the art, research status, refrigerants, and application potentials, 6 2018.

[4] Florian Kaufmann, Ludwig Irrgang, Christopher Schifflechner, and Hartmut Spliethoff. Fast and accurate modelling of twin-screw compressors: A generalised low-order approach. *Applied Thermal Engineering*, 257:124238, 12 2024.

[5] Florian Kaufmann, Hartmut Spliethoff, and Christopher Schifflechner. Reversible high-temperature heat pumps for peak load coverage in geothermal heating plants: A techno-economic analysis. *Energy Conversion and Management*, 347, 1 2026.

[6] Eric W. Lemmon, Marcia L. Huber, and Mark O. McLinden. NIST Standard Reference Database 23: Reference Fluid Thermodynamic and Transport Properties-REFPROP, Version 9.1, 2013.

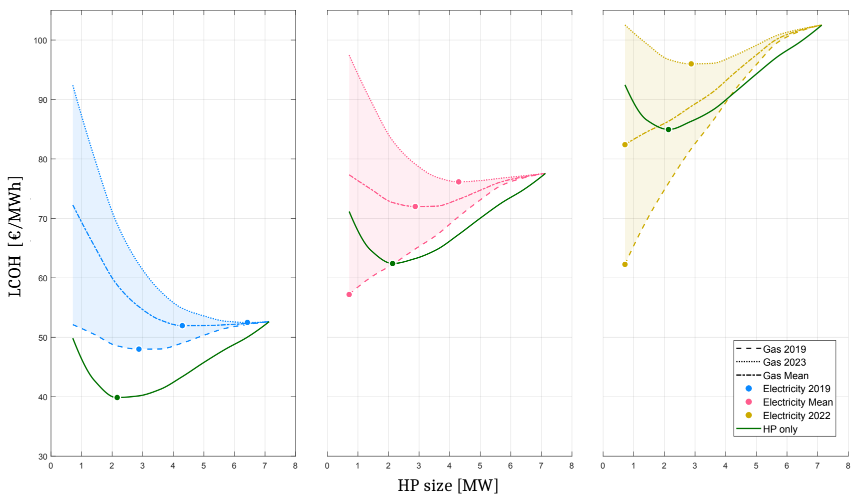

Figure 5: Influence of the natural gas and electricity price scenarios on the system LCOH as a function of the heat pump size